Thin Solid Films 518 (2010) 6304–6307

Contents lists available at ScienceDirect

Thin Solid Films

journal homepage: www.elsevier.com/locate/tsf

Effect of carrier concentration on optical bandgap shift in ZnO:Ga thin films

Chang Eun Kim [a], Pyung Moon [a], Sungyeon Kim [b], Jae-Min Myoung [b], Hyeon Woo Jang [c], Jungsik Bang [c], Ilgu Yun [a,*]

[a] Department of Electrical and Electronic Engineering, Yonsei University, 262, Seongsanno, Seodaemoongu, Seoul, 120-749, Republic of Korea
[b] Department of Materials Science and Engineering, Yonsei University, 262, Seongsanno, Seodaemoongu, Seoul, 120-749, Republic of Korea
[c] LG Chem, Ltd./Research Park, 104-1 Moonji-Dong, Yuseng-Gu, Daejeon 305-380, Republic of Korea

ARTICLE INFO

Available online 27 March 2010

Keywords:
ZnO:Ga thin film
Burstein–Moss effect
Bandgap narrowing
Modified BM equation
Carrier concentration

ABSTRACT

The Ga-doped ZnO thin films were deposited on glass substrate by sputtering and annealed at 350 °C in hydrogen atmosphere for 1 h. The optical bandgap of thin films showed the lower blueshift than the theoretical value of the Burstein–Moss (BM) effect. The shift of bandgap was dependent on the carrier concentration and acquired by combining the nonparabolic BM effect and bandgap narrowing (BGN). The modified BM effect equation was proposed to substitute the nonparabolic BM effect and BGN. The exponent in the modified BM equation was affected by carrier concentration and it was decreased with carrier concentration.

1. Introduction

Transparent conductive oxide (TCO) films have been widely used for electrodes in optoelectronic devices such as solar cells, organic light emitting diodes and flat-panel display devices. Various oxide materials including CdO, In_2O_3, SnO_2 and ZnO have been studied for TCO applications [1]. Among them, Sn-doped indium oxide (ITO) thin films have been practically commercialized due to its low resistivity and high transparency in visible range [2]. However, ZnO is recently emerged to be an alternative material for ITO, because ZnO has the advantage such as low cost, non-toxicity and high stability in hydrogen plasma. ZnO is also a wide bandgap semiconductor (3.37 eV) with high exciton binding energy (60 meV) and its electrical and optical properties may be changed by doping with group-III impurities such as Ga, In and Al [3–5]. Moreover, doped ZnO thin films show the high conductance and high transparency by thermal annealing [6,7].

It was well known that bandgap widening and narrowing occurred in heavily doped semiconductors [8,9]. Bandgap widening is referred to as the Burstein–Moss (BM) effect, the conduction band becomes significantly filled at high doping concentration and the lowest energy states in the conduction band are blocked. Bandgap narrowing (BGN) has been explained by many-body effect of free carriers on the conduction and valence bands, which is known as bandgap renormalization. Many research groups have been suggested the equation to define the bandgap shift in highly doped n-type semiconductor [10–12]. Recently, it was reported that the BM effect and BGN affect to optical bandgap of semiconductor simultaneously and BGN emerges above the critical value [13]. In this paper, the electrical and optical properties of ZnO:Ga thin films are analyzed and the optical bandgap shift depending on carrier concentration is investigated. The modified BM effect equation is proposed to explain the optical bandgap shift of ZnO:Ga thin films.

2. Experimental details

ZnO:Ga thin films were prepared on glass substrate by RF magnetron sputtering method. GZO ceramics (ZnO:95 wt.%, Ga_2O_3:5 wt.%) was used as a source target. The chamber was evacuated to a base pressure of 2×10^{-6} Torr and the deposition was carried out at working pressure of 3 mTorr. Ar was used as a carrier gas. The growth temperature was maintained at room temperature and the RF sputtering power was kept at 100 W. The thickness of thin film was controlled by the deposition time with the deposition rate of 0.1 nm/s and it was in the range between 160 and 185 nm. After the deposition, thermal annealing was performed in the temperature of 350 °C in hydrogen atmosphere for 1 h. The carrier concentration of ZnO:Ga thin film was measured by the hall measurement using Van der Pauw method. The transmittance of ZnO:Ga thin film was also measured by the spectrophotometer in the wavelength range of between 270 and 800 nm.

3. Results and discussion

3.1. Optical and electrical properties

The transmission characteristics in UV–Vis-IR regions of as-deposited and annealed ZnO:Ga thin films with the thickness of

* Corresponding author. Tel.: +82 2 2123 4619; fax: +82 2 313 2879.
E-mail address: iyun@yonsei.ac.kr (I. Yun).

0040-6090/$ – see front matter © 2010 Elsevier B.V. All rights reserved.
doi:10.1016/j.tsf.2010.03.042

160 nm and 185 nm are shown in Fig. 1. The plots of $(\alpha h\nu)^2$ versus $h\nu$ of ZnO:Ga thin films are also shown in the inset of Fig. 1. When the ZnO:Ga thin films were annealed, the average transmittance was enhanced up to 85% and the absorption edge was shifted to shorter wavelength. It is indicated that the carrier concentration of the thin films was increased after annealing. The relationship between the absorption coefficient (α) and the optical bandgap of semiconductor (E_g) is described by the following equation:

$$\alpha h\nu = C\left(h\nu - E_g\right)^x, \quad (1)$$

where C is the constant, $h\nu$ is the energy of incident photons, and x is a parameter and its value is 0.5 for a direct semiconductor [14]. The optical bandgap was obtained by the intercept of the linear region in plotting $(\alpha h\nu)^2$ versus $h\nu$ [14]. The optical bandgap and the carrier concentration depending on the thickness of ZnO:Ga thin film were summarized in Table 1. After the annealing process, the optical bandgap and the carrier concentration were increased. The increase of carrier concentration by annealing was explained by the generation of oxygen vacancies and interstitial Zn metals due to thermal energy [15]. The increase of the optical bandgap was explained by BM effect due to the increased carrier concentration. However, the previous research reported that BM equation does not fit to the bandgap shift in ZnO:Ga thin films [16].

3.2. BM effect and bandgap narrowing

The experimental data of the bandgap shifts in ZnO:Ga thin films are presented in Fig. 2(a). After the annealing, the dramatic increase of the optical bandgap was observed at the position between 1.5×10^{21}/cm^3 and 1.8×10^{21}/cm^3 and the bandgap shift was decreased slightly at the region above 3×10^{21}/cm^3. It is denoted that the optical bandgap was affected by BGN as well as BM effect. The various effect plots for the bandgap shift to consider the BM effect and BGN are shown in Fig. 2(b). In the model of BM effect, the bandgap widening in n-type semiconductor with parabolic band is given by the following equation:

$$\Delta E^{BM} = \frac{h^2}{8\pi^2 m^*}\left(3\pi^2 n\right)^{2/3}, \quad (2)$$

where ΔE^{BM} is the blueshift of the optical bandgap, h is Plank's constant, n is the carrier concentration, and m^* is the electron effective mass in the conduction band [8]. The dotted line in Fig. 2(b) was acquired by Eq. (2). The result shows that the theoretical values of BM effect were larger than the experimental data. It is due to the variation of electron effective mass which is dependent on the carrier concentration at degenerate semiconductor because of the

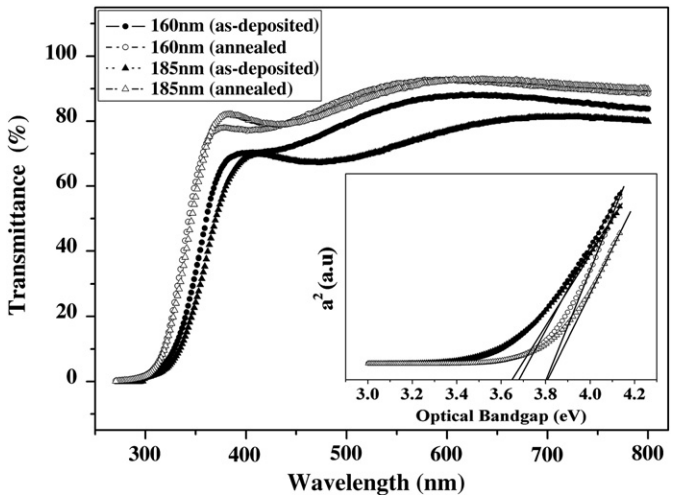

Fig. 1. The transmittance in UV–Vis-IR regions of ZnO:Ga thin films. The inset shows the plot of $(\alpha h\nu)^2$ versus $h\nu$.

Table 1
The experimental data of the optical bandgap and carrier concentration in ZnO:Ga thin films.

Thickness (nm)	N (cm^{-3})	Optical Bandgap (eV)	Process
160	1.45×10^{21}	3.672	as-deposited
170	8.14×10^{20}	3.659	
173	3.82×10^{20}	3.648	
185	4.94×10^{20}	3.651	
160	1.83×10^{21}	3.801	annealed
170	2.01×10^{21}	3.818	
173	3.95×10^{21}	3.799	
185	3.69×10^{21}	3.805	

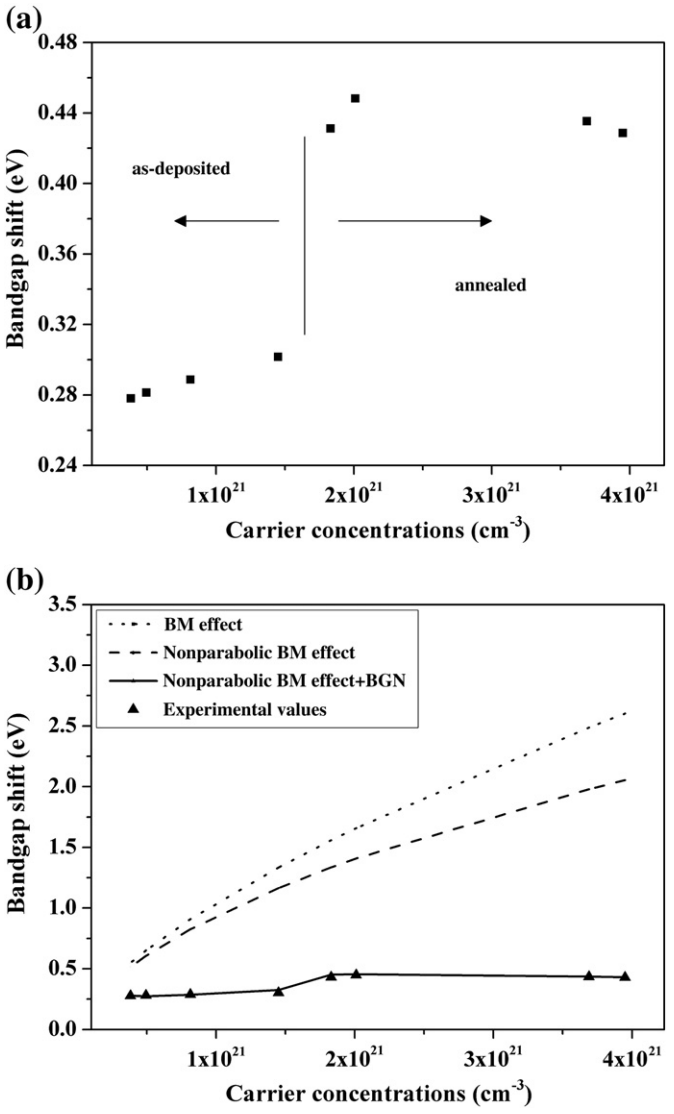

Fig. 2. (a) The experimental bandgap shift with carrier concentration in ZnO:Ga thin films and (b) the function of bandgap shift on carrier concentration. The dotted line, the dashed line, and solid line were the result of theoretical BM effect, the nonparabolic BM effect, and the nonparabolic BM effect and BGN, respectively.

nonparabolic conduction band [13]. The electron effective mass in our study was proportional to $n^{2/3}$ and was expressed by [13]:

$$(m^*)_{\text{non}} = m^*\left[1 + D\frac{h^2}{2\pi^2 m^*}(3\pi n)^{2/3}\right]^{1/2}, \quad (3)$$

where D is a constant. By replacing the m^* in Eq. (2) with $(m^*)_{\text{non}}$, the nonparabolic BM effect was acquired and represented by the dashed line in Fig. 2(b).

The difference between the theoretical values of nonparabolic BM effect and the measured data was explained by BGN. Here, the many-body interaction effects were the main mechanism of BGN where it occurs either between free carriers or between free carriers and ionized impurities. In n-type semiconductor, electron–electron interactions, electron–hole interactions, and electron–donor interactions are effective terms and described by the following equation [9]:

$$\Delta E^{\text{BGN}} = \frac{1.83\Lambda}{r_s N_b^{1/3}}R + \frac{0.95}{r_s^{3/4}}R + \frac{\pi}{2r_s^{3/2}N_b}\left(1 + \frac{m^*_{\text{min}}}{m^*_{\text{maj}}}\right)R, \quad (4)$$

where R is the Rydberg energy, Λ is the correction factor which accounts for anisotropy of the bands, N_b is the number of equivalent band extrema and $m^*_{\text{min}}/m^*_{\text{maj}}$ is the ratio of the minority carrier effective mass to the majority carrier effective mass. Here, r_s is the average distance between electrons and expressed as the following equation:

$$r_s = \left(\frac{3}{4\pi}\right)^{1/3} n^{-1/3} \times (a^*)^{-1}, \quad (5)$$

where a^* is the effective Bohr radius.

The solid line in Fig. 2(b) was the result of considering the nonparabolic BM effect and BGN, which can agree well with the experimental data. Here, the first and last terms of Eq. (4) were considered in the region under $1.5\times10^{21}/\text{cm}^3$ and the first term was solely effective in the region above $1.5\times10^{21}/\text{cm}^3$. The second term, which was related with the electron–hole interactions, was not considered because the all samples were highly n-type and has very low hole concentration. When the carrier concentration was lower than the critical value, the electron–donor interactions as well as the electron–electron interactions should be considered and the bandgap shift was dependent on the terms of $n^{2/3}$, $n^{1/3}$, and $n^{1/2}$. However, it is observed that the carrier concentration in the annealed samples was over the critical values due to the carrier generation such as oxygen vacancies and zinc interstitials [17]. Since the number of the generated electrons is extremely larger than the number of donors in the annealed sample, the effect of donor is relatively lower than that of electrons. Therefore, the electron–donor interactions were neglected and electron–electron interactions were dominant. As a result, the bandgap shift was related with $n^{2/3}$ and $n^{1/3}$.

3.3. Modified BM effect

The modified BM effect is proposed to substitute the combination of nonparabolic BM effect and BGN. The exponent in Eq. (2) is calculated by using the experimental data and it is shown in Fig. 3(a). The label of y-axis in Fig. 3 is the numerator of exponent when the denominator of exponent is considered to be 60 as a reference value. The exponent in theoretical BM effect is fixed at 2/3. Based on the results in this study, the exponent was dependent on carrier concentration. It was decreased with carrier concentration up to $1.5\times10^{21}/\text{cm}^3$ and it was abruptly increased where carrier concentration is near $2\times10^{21}/\text{cm}^3$ and then re-decreased with carrier concentration up to $4\times10^{21}/\text{cm}^3$. The decrease of exponent was attributed to the bandgap narrowing by the many-body effect. The reason of abrupt increase in the region of $1.5\times10^{21}/\text{cm}^3$ was that the electron–electron interactions term in

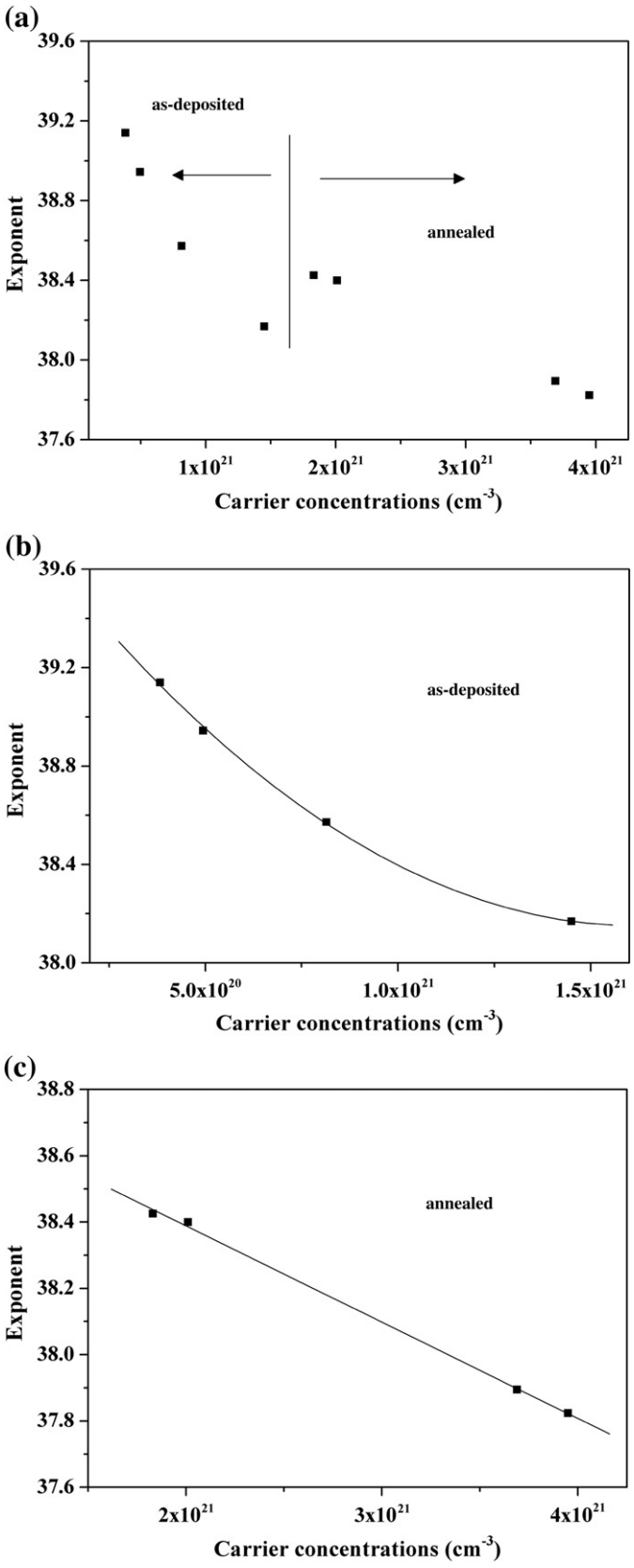

Fig. 3. (a) The calculated exponent in the modified BM effect by using the experimental data, (b) the exponent and quadratic polynomial equation in the modified BM effect in the region under $1.5\times10^{21}/\text{cm}^3$, and (c) the exponent and linear equation in the modified BM effect in the region above $1.5\times10^{21}/\text{cm}^3$.

Table 2
Summary of constants in the modified BM effect equation.

when $n < 1.5\times10^{21}/cm^3$		when $n > 1.5\times10^{21}/cm^3$	
a	39.83/60	α	38.97/60
b	-2.06×10^{-21}/60	β	-2.90×10^{-22}/60
c	6.37×10^{-43}/60		

many-body effect was dominant above critical point. Fig. 3(b) and (c) show the equation of exponent in BM effect depending on the carrier concentration. The modified BM effect equations were represented by the following equations:

$$\Delta E^{\mathrm{BM}} = \frac{h^2}{8\pi^2 m^*}\left(3\pi^2 n\right)^{\left(a + bn + cn^2\right)}, \text{for } n < 1.5\times10^{21}/\mathrm{cm}^3 \quad (6)$$

$$\Delta E^{BM} = \frac{h^2}{8\pi^2 m^*}\left(3\pi^2 n\right)^{(\alpha + \beta n)}, \quad for\ n > 1.5\times10^{21}/cm^3 \quad (7)$$

where a, b, c, α, and β are constants and summarized in Table 2. In the equations for the modified BM effect, the variation of each exponent term was due to the change of significant interactions in many-body effect. The carrier concentration in ZnO:Ga thin films is originated from the oxygen vacancies, the interstitial Zn metal and the donor electrons of Ga. Therefore, the electron–electron and the electron–donor interactions were effective in the as-deposited thin films under $1.5\times10^{21}/cm^3$. As a result, the exponent term of the modified BM equation was represented by quadratic polynomial function of carrier concentration. Above mentioned, the increase of carrier concentration after the annealing was due to the increase of oxygen vacancies and zinc interstitials [15]. The number of electrons generated by oxygen vacancies and zinc interstitials was extremely larger than the number of donors. Therefore, the electron–electron interactions were dominant compared with the other interactions. Consequently, the exponent term of the modified BM equation was described by linear function of carrier concentration.

4. Conclusion

In summary, ZnO:Ga thin films were deposited on glass substrate by sputtering at room temperature and annealed in the temperature 350 °C in hydrogen atmosphere for 1 h. Based on the results, the blueshift of the optical bandgap was observed but it was smaller than the theoretical value of the BM effect. The experimental data was then explained by BM effect considering the nonparabolic conduction band and BGN due to many-body effect. In addition, the modified BM effect equation was proposed and described at which the exponent was dependent on carrier concentration. It can be concluded that the electron–electron interactions and the electron–donor interactions of BGN were considered in the region under $1.5\times10^{21}/cm^3$ and the electron–electron interactions was solely effective in the region above $1.5\times10^{21}/cm^3$.

Acknowledgements

This work was supported by the Korea Science and Engineering Foundation (KOSEF) grant funded by the Korea government (MOST) (No. R01-2007-000-20143-0) and the grant from the "Strategic Technology Development Programs (No. 10032091)" of the Ministry of Knowledge Economy (MKE) of Korea.

References

[1] C.G. Granqvist, Sol. Energy Mater. Sol. Cells 91 (2007) 1529.
[2] E. Fortunato, A. Pimental, A. Gonçalves, A. Marques, R. Martins, Thin Solid Films 496 (2006) 89.
[3] V. Bhosle, A. Tiwari, J. Narayan, J. Appl. Phys. 100 (2006) 0337131.
[4] Y.R. Park, E.K. Kim, D.G. Jung, T.S. Park, Y.S. Kim, Appl. Surf. Sci. 254 (2008) 2250.
[5] K.H. Kim, K.C. Park, D.Y. Ma, J. Appl. Phys. 81 (1997) 7764.
[6] J.K. Sheu, K.W. Shu, M.L. Lee, C.J. Tun, G.C. Chi, J. Electrochem. Soc. 154 (2007) H521.
[7] X. Yu, J. Ma, F. Ji, Y. Wang, X. Zhang, H. Ma, Thin Solid Films 483 (2005) 296.
[8] I. Hamberg, C.G. Granqvist, Phys. Rev. B 30 (1984) 3240.
[9] S.C. Jain, J.M. McGregor, D.J. Roulston, J. Appl. Phys. 68 (1990) 3747.
[10] H.Y. Xu, Y.C. Liu, R. Mu, C.L. Shao, Y.M. Lu, D.Z. Shen, X.W. Fan, Appl. Phys. Lett. 86 (2005) 123107.
[11] K.J. Kim, Y.R. Park, Appl. Phys. Lett. 78 (2001) 475.
[12] T. Makino, Y. Segawa, S. Yoshida, A. Tsukazaki, A. Ohtomo, M. Kawasaki, H. Koinuma, Jpn. J. Appl. Phys. 44 (2005) 7275.
[13] J.G. Lu, S. Fujita, T. Kawaharamura, H. Nishinaka, Y. Kamada, T. Ohshima, Z.Z. Ye, Y.J. Zeng, Y.Z. Zhang, L.P. Zhu, H.P. He, B.H. Zhao, J. Appl. Phys. 101 (2007) 083705.
[14] I.K. El Zawawi, R.A. Abd Alla, Thin solid films 339 (1999) 314.
[15] G.J. Fang, D.J. Li, B.L. Yao, Phys. Status Solidi (a) 193 (2002) 139.
[16] J.D. Ye, S.L. Gu, S.M. Zhu, S.M. Liu, Y.D. Zheng, R. Zhang, Y. Shi, Appl. Phys. Lett. 86 (2005) 192111.
[17] B.-Y. Oh, M.-C. Jeong, D.-S. Kim, W. Lee, J.-M. Myoung, J. Crystal Growth 281 (2005) 475.